

## Heterogeneity of multiwalled carbon nanotubes based on adsorption of simple aromatic compounds from aqueous solutions

Przemysław Podkościelny<sup>a,\*</sup>, Ajna Tóth<sup>b</sup>, Barbara Berke<sup>b</sup>,  
Krisztina László<sup>b</sup>, Krzysztof Nieszporek<sup>a</sup>

<sup>a</sup>*Faculty of Chemistry, Department of Theoretical Chemistry, Maria Curie-Skłodowska  
University, pl. M. Curie-Skłodowskiej 3, 20-031 Lublin, Poland*

<sup>b</sup>*Department of Physical Chemistry and Materials Science, Budapest University of  
Technology and Economics, H-1521 Budapest, Hungary*

### Abstract

The surface heterogeneity of multiwalled carbon nanotubes (MWCNTs) is studied on the basis of adsorption isotherms from dilute aqueous phenol and dopamine solutions at various pH values. The generalized Langmuir-Freundlich (GLF) isotherm equation was applied to investigate the cooperative effect of the surface heterogeneity and the lateral interactions between the adsorbates. The theoretical isosteric heats of adsorption were obtained assuming that the heat of adsorption profile reveals both the energetic heterogeneity of the adsorption system and the strength of the interactions between the neighboring molecules. The adsorption energy distribution (AED) functions were calculated by using algorithm based on a regularization method. The great advantage of this method is that the regularization makes no assumption about the shape of the obtained energy distribution functions. Analysis of the isosteric heats of adsorption for MWCNTs showed that the influence of the surface heterogeneity is much stronger than the role of the lateral interactions. The most typical adsorption heat is 20-22 kJ/mol for both phenol and dopamine. After purification of nanotubes, heat value for phenol dropped to 16-17 kJ/mol. The range of the energy distribution is only slightly influenced by the surface chemistry of the nanotubes in the aqueous conditions.

*Keywords:* multiwalled carbon nanotubes; phenol; dopamine; heterogeneity; pH; heat of adsorption

\*Corresponding author

*E-mail address:* przemyslaw.podkoscielny@poczta.umcs.lublin.pl

Tel: + 48 81 5375788; Fax: + 48 81 5375685

## 1. Introduction

Increasing concern about the potential hazard of pollution by pharmaceuticals in aqueous environments has revived apprehensions with respect to the treatment of drinking water. Non-biodegradable organic, mainly aromatic, compounds cannot be eliminated by biological treatment, and they even may act as inhibitors already at low concentration. Adsorption by activated carbons (ACs) is still among the most extensively used technologies, owing to its high affinity for a wide variety of chemicals (Dąbrowski et al. 2005; Podkościelny 2008; Podkościelny and László 2007; Terzyk 2004; Deryło-Marczewska et al. 2010; Marczewski et al. 2013; Hua et al. 2012; Podkościelny and Nieszporek 2011; Soliman et al. 2013). New materials such as multiwalled carbon nanotubes (MWCNTs) also have the potential for effective removal of organic compounds like phenol, chlorophenols, nitroaromatic compounds, etc. (Sheng et al. 2010; Shen et al. 2009; Arasteh et al. 2010; Abdel Salam et al. 2010; Ji et al. 2010; Liao et al. 2008; Tóth et al. 2011; Tóth et al. 2012; Wiśniewski et al. 2012; Li et al. 2013). However the relatively large surface area and the high sorption capacity of MWCNTs are compromised by their strong hydrophobic character, which results in self assembled aggregates. The existence of energetically different surface sites can be partially attributed to such behavior. In the case of MWCNTs the adsorption may occur a) on the external surface of the nanotubes, b) in the interstitial cavities created by the nanotubes, c) in the hollow space inside the nanotubes and d) on the grooves on the periphery of the nanotube bundles (Sheng et al. 2010; Shen et al. 2009; Agnihotri et al. 2004). The heterogeneity of the nanotubes is also associated with impurities (traces of metal catalyst, amorphous carbon), dislocations, edges. Oxygen as a heteroatom is practically always present in ambient conditions. These geometrical and chemical heterogeneities generate the unique sorption properties of MWCNTs.

The adsorption mechanism of simple aromatic compounds is complex, but as suggested by the most of authors, the driving forces are “ $\pi$ - $\pi$ ” electron-donor-acceptor interactions between aromatic molecules and the polarizable graphene sheets of MWCNTs (Sheng et al. 2010; Lin and Xing 2008; Tóth et al. 2011; Pan and Xing 2008; Chen et al. 2008). Both electron-donor (e.g.,  $-\text{OH}$ ,  $-\text{NH}_2$ ) and electron-acceptor (e.g.,  $-\text{NO}_2$ ,  $-\text{Cl}$ ) groups on benzene can increase the adsorption on CNTs (Woods et al. 2007; Star et al. 2003). The  $-\text{OH}$  group as a strong electron-donating group makes the benzene ring(s) electron rich, thus allowing the compound to interact strongly with the (electron-depleted) surfaces of carbon

nanotubes. The impact of  $-NH_2$  groups is stronger than of  $-OH$  groups, as shown by comparing e.g. the adsorption of phenol and aniline or 1-naphthylamine and 1-naphthol (Sheng et al. 2010; Yang et al. 2008). Carbon nanotubes contain polarized electron-rich and -depleted sites, caused primarily by the surface defects of carbon nanotubes (Chen et al. 2008). It is difficult to identify all types of defects contained in CNTs. Lehman et al. (2011) presented a comprehensive taxonomy of defects contained in MWCNTs. The most common defects are: 1) Structural defects, responsible for curvature changes (presence of pentagons, heptagons, etc.), 2) topological defects (bond rotations, Stone-Thrower-Wales defects), 3) substitutional non-carbon atoms (impurities, doping) and 4) non- $sp^2$  carbon defects (carbon chains, interstitials, dangling bonds, open edged nanotubes and vacancies).

The presence of all these defects contributes significantly to the energetic heterogeneity of MWCNTs surfaces.

The oxidation process that is most often employed to enhance hydrophilicity introduces further oxygen-containing functional groups, particularly acidic in nature, such as carboxyls, lactones or phenols. Moreover, the accessible traces of the metal catalyst and the amorphous carbon are practically removed. All these reactions may lead to morphological changes (surface area, pore size distribution, etc.)

Owing to the variety of chemical types of active site and the delocalized electrons of the carbon network, MWCNTs, just like ACs, exhibit acid/base character (Radovic et al. 2001). Thus, changing the pH of a solution over the nanotube significantly affects their surface protonation-deprotonation processes and modifies the adsorption properties.

The main objective of the paper is to investigate the surface heterogeneity of an untreated MWCNT and of its carboxyl functionalized form when placed in contact with dilute aqueous phenol or dopamine solutions at various pH values. These contaminants are common components in waste waters. Phenol is one of the most abundantly used chemical compounds in the pharmaceutical industry, while dopamine (4-(2-aminoethyl)benzene-1,2-diol) is a neurotransmitter used in human therapy (Parkinson's disease, schizophrenia) and also in agriculture. The calculations are based on experimental data obtained from MWCNTs in equilibrium with aqueous solutions of phenol and dopamine at 20 °C (Tóth et al. 2011). We focus on the theoretical description of the adsorption process taking into account the heterogeneous character of MWCNT surfaces.

Commercial CNTs are often contaminated with impurities such as the remains of the catalyst particles, amorphous carbon and the byproducts of the primary oxidative purification.

The catalysts can be removed by non-oxidizing acid treatments. As the oxidation method used to remove the amorphous carbon is not selective, the outer walls of MWCNTs are damaged as well. The highly fractured and oxidized outer walls similar to fulvic acids often remain adsorbed on the carbon nanotube surface. Basic aqueous solutions can be used for their removal. The process is based on the electrostatic repulsion of the negatively charged carbon surface and the deprotonated fulvic acid (Wang et al. 2009).

## 2. Theoretical

### 2.1. Adsorption equilibrium

To represent the adsorption from dilute solutions of molecules on an energetically heterogeneous adsorbent surface the fundamental equation for the overall adsorption isotherm  $\theta_t$  is (Heuchel and Jaroniec 1995; Jaroniec and Madey 1988; Płaziński and Rudziński 2009a; Podkościelny 2008):

$$\theta_t(c, T) = \int_{\Omega} \theta(\varepsilon, c, T) \chi(\varepsilon) d\varepsilon \quad (1)$$

where  $\theta(\varepsilon, c, T)$  is the fractional coverage of a given class of adsorption sites, characterized by the adsorption energy  $\varepsilon$ ;  $\theta_t(c, T) = N_t / M$ , where  $N_t$  is the absolute amount of adsorbed solute, and  $M$  is the monolayer adsorption capacity;  $\chi(\varepsilon)$  is the adsorption energy distribution function;  $\Omega$  is a range of possible energy values.

The generalization of the Langmuir isotherm for the case of single-solute adsorption, taking into account lateral interactions between admolecules, and following the Fowler-Guggenheim (FG) type isotherm (Fowler and Guggenheim 1949; Rudziński et al. 1994; Marczewski 2011), is:

$$\theta(\varepsilon, c, T) = \frac{Kc \exp\left\{\frac{\varepsilon + \omega\theta}{kT}\right\}}{1 + Kc \exp\left\{\frac{\varepsilon + \omega\theta}{kT}\right\}} \quad (2)$$

where  $K$  is the equilibrium constant. The parameter  $\omega/kT$  is the product of the interaction energy between two molecules adsorbed on two nearest-neighbor adsorption sites.

The Condensation Approximation (CA) is the method most frequently used to calculate integral (1) (Jaroniec and Madey 1988; Rudziński et al. 1994; Cerofolini 1974; Płaziński and Rudziński 2009b; Nieszporek and Banach 2012). The adsorption equilibrium isotherm  $\theta_t$  on

energetically heterogeneous surfaces with patchwise topography of adsorption sites has the form:

$$\theta_t^p = \frac{\left( Kc \exp\left\{\frac{\varepsilon_0}{kT}\right\} \exp\left\{\frac{\omega}{2kT}\right\} \right)^{kT/\nu}}{1 + \left( Kc \exp\left\{\frac{\varepsilon_0}{kT}\right\} \exp\left\{\frac{\omega}{2kT}\right\} \right)^{kT/\nu}} \quad (3)$$

For random topography of adsorption sites the equilibrium isotherm is (Rudziński and Płaziński 2008; Podkościelny 2008; Podkościelny and Nieszporek 2011):

$$\theta_t^r = \frac{\left( Kc \exp\left\{\frac{\varepsilon_0}{kT}\right\} \exp\left\{\frac{\omega\theta_t^r}{kT}\right\} \right)^{kT/\nu}}{1 + \left( Kc \exp\left\{\frac{\varepsilon_0}{kT}\right\} \exp\left\{\frac{\omega\theta_t^r}{kT}\right\} \right)^{kT/\nu}} \quad (4)$$

where  $\nu$  is the heterogeneity parameter, which is proportional to the distribution width, and  $\varepsilon_0$  is the most probable value of the adsorption energy.

Superscripts  $p$  and  $r$  refer respectively to the patchwise and to the random model. Expression (4) is known as the generalized Langmuir-Freundlich (GLF) equation taking into account lateral interactions between adsorbed molecules.

## 2.2. *Isosteric heat of adsorption*

It is known that the heat of adsorption profile reveals both the energy heterogeneity of the system and the strength of the interactions between the neighboring molecules in the adsorbed phase (Rudziński et al. 1996; Nieszporek et al. 2009; Podkościelny and Nieszporek 2011). The fundamental equation that yields expressions for isosteric heats of adsorption  $q_{st}$  has the form:

$$q_{st} = -k \left( \frac{\partial \ln c}{\partial (1/T)} \right)_{N_t} \quad (5)$$

The simplest method of obtaining a theoretical expression for  $q_{st}$  is to transform the appropriate isotherm equation for  $\ln c$  and to differentiate with respect to  $(1/T)$ . We therefore rewrite the isotherms Eqs. 3 and 4 as follows:

$$cK \exp\left\{\frac{\varepsilon_0}{kT}\right\} = \left(\frac{\theta_t^p}{1-\theta_t^p}\right)^{\nu/kT} \exp\left\{-\frac{\omega}{2kT}\right\} \quad (6)$$

and

$$cK \exp\left\{\frac{\varepsilon_0}{kT}\right\} = \left(\frac{\theta_t^r}{1-\theta_t^r}\right)^{\nu/kT} \exp\left\{-\frac{\omega\theta_t^r}{kT}\right\} \quad (7)$$

Combination of Eqs. 5 and 6 leads to  $q_{st}$  for the surface characterized by patchwise topography:

$$q_{st}^p = q_{st,0}^p - \nu \ln \frac{\theta_t^p}{1-\theta_t^p} + \frac{\omega}{2} \quad (8)$$

where

$$q_{st,0} = k \left( \frac{\partial \ln K'}{\partial (1/T)} \right)_{N_i} \quad (9)$$

and  $K' = K \exp\{\varepsilon_0/kT\}$ .

The parameter  $q_{st,0}$ , the so-called “non-configurational” isosteric heat, shifts the heat curves along the ordinate axis.

When the adsorption sites with different energies are distributed randomly on the surface, the isosteric heat of adsorption has the form:

$$q_{st}^r = q_{st,0}^r - \nu \ln \frac{\theta_t^r}{1-\theta_t^r} + \omega\theta_t^r \quad (10)$$

The major advantage of this calculation is that the above expressions specifying the isosteric heat of adsorption and the adsorption isotherm equations both use the same parameters.

### 2.3. Calculation of adsorption energy distribution (AED) functions

The AED function fundamentally describes heterogeneous properties of adsorbents. To find this function the Fredholm integral equation of the first kind must be solved. To avoid distorted results the regularization method is employed (von Szombathely et al. 1992; Heuchel et al. 1993). It should be emphasized that the regularization method makes no assumption about the shape of the energy distribution functions.

For adsorption from dilute aqueous solutions, the total fractional coverage of the solute  $\theta_t(c)$  in the surface phase may be expressed as (Heuchel and Jaroniec 1995; Heuchel et al. 1993):

$$\theta_t(c) = \frac{N_t}{M} = \int_{\varepsilon_{\min}}^{\varepsilon_{\max}} \frac{\Phi x \exp(\varepsilon / kT)}{1 + \Phi x \exp(\varepsilon / kT)} \chi(\varepsilon) d\varepsilon \quad (11)$$

where  $\Phi = \Phi(c, \theta_t)$  is a model-dependent function,  $x = c/c_s$ , where  $c_s$  is the solubility of the solute in water.

The program INTEG based on the regularization method was used for inverting Eq. 11 with respect to the energy distribution function  $\chi(\varepsilon)$  (von Szombathely et al. 1992; Heuchel and Jaroniec 1995; Dąbrowski et al. 2005; Podkościelny et al. 2002; László et al. 2003; László et al. 2006; Podkościelny and László 2007). Eq. 11 can be written in a more general form:

$$g(y) = \int_{z_{\min}}^{z_{\max}} A(z, y) f(z) dz \quad (12)$$

$g(y)$  is a known function; the integral kernel  $A(z, y)$  represents the local isotherm of Eq. 11 and  $f(z)$  denotes the unknown AED function. Regularization consists in replacing the problem of minimizing the ordinary functional  $\|Af - g\|^2$  by another functional that prevents intense oscillations of the AED function. This can be done by adding an additional term to the minimization functional, i.e.:

$$Q = \|Af - g\|^2 + \gamma \int_{z_{\min}}^{z_{\max}} f^2(z) dz \quad (13)$$

where,  $\gamma$  is the regularization parameter, which is a means of weighting both terms in Eq. 13.

### 3. Experimental

#### 3.1. Materials

Multi-walled carbon nanotubes, pristine (CNT-P) and a carboxyl functionalized (CNT-COOH) form, were purchased from Chengdu Organic Chemicals Co., Ltd., Chinese Academy

of Sciences (purity >95 (m/m)%). Their nominal external and internal diameters are 10-20 and 5-10 nm, respectively, and their length is 10-30  $\mu\text{m}$ . According to the manufacturer, the functionalized nanotube contains 2 m/m% COOH. The MWCNTs were purified with aqueous HCl solution to remove accessible traces of the catalyst (Bendjemil et al. 2004). Fulvic acid impurities were removed by the treatment proposed by Wang et al (Wang et al. 2009). The purified samples are denoted as CNT-PC and CNT-COOHC, respectively.

### 3.2. Characterization methods

High resolution transmission electron micrographs (HRTEM) were taken with a FEI Tecnai F20 transmission electron microscope operating at 120 kV. Samples for TEM investigations were produced by drop-casting the product dispersions on copper grids coated with holey carbon film. Nitrogen adsorption/desorption isotherms were measured at 77 K, using a Nova 2000e (Quantachrome, USA) computer controlled apparatus. The samples were evacuated at 293 K for 24 hours. The apparent surface area  $S_{\text{BET}}$  was obtained from the BET model. The total pore volume  $V_{0.95}$  was calculated from the amount of nitrogen vapour adsorbed at a relative pressure close to 0.95, on the assumption that the pores are then filled with liquid nitrogen. From  $S_{\text{BET}}$  and the total pore volume  $V_{0.95}$  an average pore width  $d_{\text{ave}}$  ( $=2V_{0.95}/S_{\text{BET}}$ ) was derived. The Quantachrome Data Acquisition and Reduction program (version 10.0) was used for the analysis. X-ray photoelectron spectroscopy (XPS) was used to determine the surface composition in dry state. Acid-base properties in aqueous medium were revealed by potentiometric titration in the pH range 3-10 (László et al, 2003b). The initial pH was measured before the titration started.

### 3.3. Adsorption isotherms from dilute aqueous solutions

For the phenol and dopamine uptake measurements, equilibrium adsorption data from phenol and dopamine solutions dissolved in 0.1 M aqueous NaCl solution were obtained at 20 °C. The initial pH values of the aqueous solutions were set to pH=3 and pH=11 with HCl and NaOH solution, respectively, prior to addition of the nanotubes. A third set of each tube was investigated without setting the pH (initial pH of the phenol and dopamine solutions was 5.2 and 5.3, respectively). Further details (contact time, analysis conditions, etc.) are given in



Tóth et al. 2011. Selected physico-chemical data of phenol and dopamine are shown in Table 1.

#### 4. Results and discussion

The as received commercial MWCNT (CNT-P) and its carboxyl functionalized form (CNT-COOH) were characterized by high resolution transmission electron microscopy (HRTEM), small angle X-ray scattering (SAXS), nitrogen adsorption (77 K), potentiometric titration, and electrophoretic mobility (Tóth et al. 2011). Their internal diameter is between 2-10 nm for CNT-P and 4-13 nm for CNT-COOH, respectively. It was shown by HRTEM that the MWCNTs contain 5-30 walls (Figures S1-S3, Supplementary Material). Some of the internal bores contained traces of the catalyst. The density of the concentric graphene layers decreases towards the outer layer of the nanotubes, the surface of which is rough. SAXS measurements confirmed the HRTEM results. The textural characteristics derived from nitrogen adsorption measurement are listed for both nanotubes in Table S1 (Tóth et al. 2011) (Supplementary Material). The low values of the apparent BET surface area show that the internal boreholes of the nanotubes, which would significantly enhance the nitrogen adsorption at low relative pressure, are hardly accessible. Beside potential kinetic hindrance the bamboo-like structure blocking the access to the inner surface, the surface roughness and micropores forming at the junction of the CNTs are the source of the discrepancy between the geometrical and nitrogen adsorption data.

X-ray photoelectron spectroscopy (XPS) was used to determine the surface composition in dry state. The O/C ratio was 0.018 and 0.051 for the as-received pristine and the oxidized nanotubes, respectively. The potentiometric titration curves revealed the differences in the acid-base properties of the nanotubes. The values of the net proton surface excess of CNT-P and CNT-COOH, which are positive at pH=3 for both types of tube, decrease almost linearly with a slope of -0.014 and -0.057 mM/g per unit increase of pH, respectively. The point of zero net proton surface excess ( $\text{pH}_{\text{PZNPSE}}$ ) is 6.1 and 3.8, respectively. The narrow hysteresis loop of the cyclic titration curves reveals that diffusion has a very limited role in the proton exchange process in both of the tubes (László et al. 2003b).

All the experimental adsorption isotherms from aqueous phase belong to type L in Giles's classification (Giles et al. 1974).

The adsorption of phenol on purified MWCNTs (distinguished by “C”) (Tóth et al. 2012) was also studied in order to reveal the potential effect of the contaminants (e.g., catalysts and fulvic acid). Nitrogen adsorption data show that the surface area and the porosity of the MWCNTs were practically not affected by the purification (Table S1, Supplementary Material). Neither structural damage nor any change of the inner and the outer diameter was observed by HRTEM. Nevertheless, the surface composition of the purified MWCNT changed due to the complex purification as reflected by the depletion of the O/C ratio to 0.013 and 0.035 in CNT-PC and CNT-COOHC, respectively.

#### 4.1. Equilibrium adsorption

##### 4.1.1. Adsorption of phenol from dilute aqueous solution

For the geometrically disordered and chemically heterogeneous surface of MWCNTs, which can be characterized by a random distribution of the adsorption sites, the GLF equation (Eq. 4) was employed to fit the experimental data.

The adsorption isotherms obtained with aqueous phenol solutions on CNT-P and oxidized CNT-COOH at the different pH values are presented in Fig. S4 (Supplementary material). The symbols in the figure denote the experimental data (Tóth et al. 2011), while the lines are the theoretical isotherms calculated from Eq. 4. The results of the fit are summarized in Table 2. This table includes the values of monolayer capacity  $M$  and the equilibrium constant  $K' = K \exp\{\varepsilon_0 / kT\}$ . The parameter  $kT/v$  characterizes the energetic heterogeneity of the surface. The parameter  $\omega/kT$  represents the average strength of the lateral interactions in the monolayer. The surface area available for one adsorbate molecule  $a_{GLF}$  is calculated based on  $M$  values from the GLF model. The quality of the fit of Eq.4 to the experimental data is described by the following *Error* function (residual sum of squares):  $Error = \sum (\exp - theor)^2$ . The last column lists the surface coverage by the adsorbate relative to the surface area  $S_{BET}$ .

Both the nanotube surface and the phenol molecule are influenced by the pH conditions. At pH = 3, phenol is in its molecular form (pH < pK<sub>a, phenol</sub>=9.89). The nanotubes are also protonated. The functional groups of acidic character are uncharged, the delocalized  $\pi$  electrons, however, attract protons and thus the surface gains a positive charge. These conditions seem to favor the adsorption of phenol, since the highest monolayer capacity

occurs for both CNT-P and CNT-COOH at pH 3. It seems likely that the aromatic ring of the phenol could be attracted by the protonated nanotube surface. The lowest values of  $kT/v$  shown at pH = 3 imply that both nanotube surfaces have the most heterogeneous character in this medium (we recall, for the ordinary Langmuir equation the  $kT/v$  value is equal one – purely homogeneous surface).

A positive value of  $\omega/kT$  in Eq. 4 means that the lateral interactions have an attractive character. The values in Table 2 show that this is maximum at pH=3 again for both nanotubes. The higher population of phenol molecules in the surface monolayer may be responsible for the strongest lateral interactions. These interactions are however disturbed by the acidic groups decorating the CNT-COOH sample, as revealed by comparison with the corresponding  $\omega/kT$  values.

With increasing pH the interaction weakens (protonation is suppressed) and the monolayer capacity decreases slightly. In the case of CNT-P both the adsorption capacity and the lateral interaction diminish in the “non-set” pH conditions, where the equilibrium pH=6.7. The lack of protons attracted by the delocalized  $\pi$  electrons of the surface could be responsible for a more uniform surface site distribution ( $kT/v$  is close to 1).

At nominal pH =11 the phenol forms phenolate anions, while the surface functional groups are either neutral or negatively charged. The electrostatic repulsion between the identical charges reduces the adsorption capacity. This tendency is more marked for CNT-COOH (Fig. S4 (b)), which has a higher pH sensitivity for its acidic functional groups. This also weakens the lateral interactions. It is worthwhile to note that the most homogeneous surface appears with the “not set (5.2)” pH conditions for CNT-P and at the highest pH for CNT-COOH.

It can be assumed that in the case of dilute solutions the mechanism of adsorption on the nanotubes is similar to ACs, i.e., the total surface is covered by a monolayer of phenol (Stoeckli et al. 2001; Fernandez et al. 2003). Water is always adsorbed preferentially by the oxygen-containing surface groups (Tóth and László 2012). The adsorbed water molecules then act as nuclei for the formation of larger H-bonded water clusters. As a result, the associated water can prevent migration of the phenol molecules to the hydrophobic parts of the surface and effectively reduce their uptake. This interpretation explains why the values of  $a_{GLF}$  are much larger than the cross-sectional area of phenol (0.30-0.42 nm<sup>2</sup>) (László and Szűcs 2001). It is worthwhile to mention that, in the case of a microporous polymer-based AC with a similar surface composition (O/C ratio 0.045), the surface area available for a phenol

molecule was, respectively, 0.872, 0.750 and 1.516 nm<sup>2</sup> at nominal pH 3, non-set and 11 (László et al. 2003). The discrepancy in the occupied surface area and the pH dependence of the two systems may be explained by the pore filling mechanism in the case of AC, and possible differences in the distribution of the various functional groups.

Only 8.6 - 15.0 % (last column, Table 2) of the  $S_{BET}$  surface area is available for phenol. Smaller molecules (0.162nm<sup>2</sup> for N<sub>2</sub> at 77 K) have a chance to reach adsorption sites that are inaccessible to larger adsorbate molecules. Interstitial cavities created by the nanotubes are of limited access for phenol. Aggregation of nanotubes limits the availability of the adsorption sites for phenol too. As mentioned earlier, associated water can prevent movement of the phenol molecules to the hydrophobic parts of the surface, reducing their uptake. Furthermore, different surface defects of carbon nanotubes affect the adsorption conditions.

The adsorption capacity increased on the purified MWCNT (Table 3, Fig. S5), and  $a_{GFL}$  accordingly decreased. The purification also affected the interaction parameter  $K'$ , which dropped significantly. The increased lateral interaction reflects that the interaction between the adsorbed molecules became stronger. The behavior of the heterogeneity parameter after purification depends on the surface chemistry of the carbon nanotube. In case of CNT-P, the heterogeneity parameter decreases after acid-base washing, but in case of CNT-COOH,  $kT/v$  increases after purification.

Lateral interactions in the Fowler-Guggenheim model are averaged by the so-called mean field approximation. Assuming a random distribution of adsorption sites, the additional force field acting on an adsorbed molecule (from the neighboring molecules) depends on the average coverage of the neighboring sites, which is equal to  $\theta_i(c,T)$ . The values of interaction energy  $\omega$  have very low values (Table 2, 3), not exceeding 1500 J/mol in the case of purified MWCNTs (Table 3). This range of energy indicates the dispersion interactions. This interaction is relatively long range, extending to distances of 0.3-0.5 nm. It follows that the very small energy values in our case indicate the interaction of molecules that are (on average) at a distance close to 0.5 nm.

#### 4.1.2. Adsorption of dopamine from dilute aqueous solution on MWCNTs

The adsorption isotherms of dopamine from aqueous solutions on CNT-P and CNT-COOH surface at pH 3 and “not set (5.3)” pH are displayed in Fig. S6 (Supplementary material) (Tóth et al. 2011). The lines are the theoretical isotherms estimated from the GLF

model (Eq. 4). The results of the GLF calculations are summarized in Table 4. As self-polymerization of dopamine takes place in high pH, isotherms at pH=11 were not measured (Postma et al. 2009).

CNT-P adsorbs more dopamine when the pH is not set 5.3 (Fig. S6 (a)). The mechanism of dopamine adsorption on MWCNTs is as follows. At pH 3, dopamine (weak base,  $pK_a=8.93, 10.6$  (Ishimitsu et al. 1978)) is in the form of protonated cations. The surface of CNT-P is also positively charged,  $pH < (pH_{PZNPSE}=6.1)$ . Increasing the pH suppresses the protonation and thus the electrostatic repulsion weakens, resulting in a higher dopamine uptake. The lateral interactions ( $\omega/kT$ ) are stronger for adsorption at “not set (5.3)” pH. Naturally, as there is a higher number of dopamine molecules in the surface monolayer the attraction between the molecules is stronger.

CNT-COOH adsorbs more dopamine than does CNT-P. The dispersive interactions are enhanced if the experiments are carried out near the  $pH_{PZNPSE} = 3.8$  at which the repulsive interactions between the surface functionalities and molecules are minimized. When pH is not set, CNT-COOH is already deprotonated, exhibiting a negative surface charge. The positively charged dopamine is then strongly attracted by the surface.

The presence of water in the adsorbed layer is confirmed by the fact that the surface area available for a single dopamine molecule  $a_{GLF}$  is significantly larger than the cross-sectional area of dopamine ( $0.47 \text{ nm}^2$ , (Tóth et al. 2011)) in all the systems.

Values of surface coverage  $\theta$  (last column, Table 4) show that 22.1 - 33.9 % of the  $S_{BET}$  surface area is available for dopamine. The increased adsorption of dopamine compared to phenol is due to the nature of the dopamine molecule. Higher number of substituents in dopamine and presence of the amino group (basic character) cause stronger interactions with the surface. This is particularly evident in the case of adsorption on the CNT-COOH.

#### 4.2. Heat effects of adsorption

The analysis of the enthalpic effects accompanying the adsorption phenomenon can provide valuable information on an adsorption system. A decrease in the isosteric heat of adsorption with adsorbate loading is typical of adsorbents with energetically heterogeneous surfaces. Conversely, an increase of the heat curves is characteristic of homogeneous surfaces and cooperative interactions between the admolecules. Finally, if the heat of adsorption is independent of the amount adsorbed, this indicates a balance between the strength of the

adsorbate - adsorbate interactions and the degree of heterogeneity of the adsorbent - adsorbate system (Podkościelny and Nieszporek 2011; Rudziński et al. 1996; Nieszporek et al. 2009).

The quantities  $kT/\nu$  and  $\omega/kT$  obtained from the analysis of the experimental isotherms by Eq. 4 were used to calculate the theoretical isosteric heats of adsorption  $q_{st}$  according to Eq. 10. The calculations were carried out using the parameters listed in Tables 2-4, respectively. Figures 1-3 show the theoretical isosteric heats of adsorption from the aqueous solutions of phenol (Figs 1, 2) and dopamine (Fig. 3).

In all the systems analyzed, the isosteric heat decreases with increasing surface coverage, i.e., energy heterogeneity plays a more substantial role than the lateral interaction between the adsorbed molecules. The influence of the initial pH is the most obvious in the CNT-COOH – dopamine system.

The calculated heats of adsorption are displayed as decreasing from positive to negative values, because the results of our calculations are presented as  $(q_{st} - q_{st,0})$  vs.  $\theta_t$ , since the values of the parameter  $q_{st,0}$  were not available.

#### 4.3. Analysis of adsorption-energy distribution (AED) functions

Figures 4, 5 show the adsorption energy distribution functions, obtained by inverting Eq. 11, for original CNT-P and modified CNT-COOH at different pH values. Numerically stable AED functions were obtained with the regularization parameter  $\gamma = 0.001$ . In Fig. 4A, which shows the adsorption energy distribution functions for phenol on CNT-P at different values of pH, the single peak of the energy distribution function for “not set pH (5.2)” exhibits a maximum at about  $\varepsilon^{\max} = 19.47$  kJ/mol. That for pH 11 is lower, broader and shifted towards slightly higher energy ( $\varepsilon^{\max} = 20.79$  kJ/mol) than the “not set (5.2)” pH peak. The lowest peak, covering the widest range of adsorption energies, is for the pH 3 solution. The direction of these changes correlates well with the order of heterogeneity parameters  $kT/\nu$  from the GLF equation. Otherwise we know that for smaller values of the heterogeneity parameter  $kT/\nu$ , the peak is slightly shifted in the direction of greater energies. Similar conclusions can be drawn from Figure 4B. With the polymer based AC mentioned earlier, the maxima of the analogous distribution peaks were at 19-20 kJ/mol (László et al. 2003).

Figure 5 shows the adsorption energy distribution functions for dopamine. The shape of the curves is different from that of phenols. The sequence of the peaks in the direction of increasing energy, however, similarly to phenol, correlates well with the sequence of the

heterogeneity parameter  $kT/\nu$  for the GLF equation. The peak is “broader” (larger  $\Delta\varepsilon$ ), i.e., the interactions between the MWCNT and the adsorbate span a wider range. The strong interactions for adsorption of dopamine on CNT-COOH for pH 3 are reflected in the wide distribution function, which extends up to ca. 60 kJ/mol.

Numerical data for the adsorption energy distribution functions for phenol and dopamine are given in Tables 5 and 6, respectively. The calculated distribution functions suggest that the most probable values of adsorption energies for the systems studied are approximately 20 - 22 kJ/mol. As already mentioned, the direction of changes of these values correlates well with the order of heterogeneity parameters.

On the purified CNT-PC and CNT-COOHC samples  $\varepsilon^{\max}$  decreased to 17.8 kJ/mol and 16.4 kJ/mol, respectively, and both peaks become narrower (Figure 6, Table 7).

## 5. Conclusions

The equilibrium adsorption isotherms from aqueous phenol and dopamine solutions were studied on two multiwall carbon nanotubes with different surface chemistry. A good fit of the generalized Langmuir-Freundlich (GLF) isotherm to the experimental data was obtained. The advantage of the model calculation is the common parameter set appearing in the equations describing equilibrium and the associated heat of adsorption. The use of this compact calculation model extends the possibilities of interpreting values obtained. For all the systems, the isosteric heat of adsorption decreases with increasing surface coverage. This indicates that in these systems energetic heterogeneity plays a more fundamental role than lateral interaction between neighboring molecules at adsorption equilibrium. The energy distribution functions are useful for comparing the heterogeneities of the different MWCNTs in the aqueous solutions, because the uncertainties in the evaluation of these functions are analogous for all the systems studied. According to the calculated AED functions the most probable values of the adsorption energies are approximately 20 - 22 kJ/mol for the systems studied. After purification of nanotubes,  $\varepsilon^{\max}$  decreased by a few kJ/mol. The purification of the MWCNTs increased the phenol uptake, but in the same time the strength of interaction ( $K'$ ) became 3-4 times weaker. The lateral interaction on both purified carbon nanotubes is significantly stronger than on the as-received ones.

## References

- Abdel Salam, M., Mokhtar, M., Basahel, S.N., Al-Thabaiti, S.A., Obaid, A.Y.: Removal of chlorophenol from aqueous solutions by multi-walled carbon nanotubes: Kinetic and thermodynamic studies. *J. Alloys Comp.* **500**, 87-92 (2010).
- Agnihotri, S., Rostam-Abadi, M., Rood, M. J.: Temporal changes in nitrogen adsorption properties of single-walled carbon nanotubes, *Carbon* **42**, 2699-2710 (2004).
- Arasteh, R., Masoumi, M., Rashidi, A.M., Moradi, L., Samimi, V., Mostafavi, S.T.: Adsorption of 2-nitrophenol by multi-wall carbon nanotubes from aqueous solutions. *Appl. Surf. Sci.* **256**, 4447-4455 (2010).
- Bendjemil, B., Borowiak-Palen, E., Graff, A., Pichler, T., Guerioune, M., Fink, J., Knupfer, M.: Elimination of metal catalyst and carbon-like impurities from single-wall carbon nanotube raw material. *Appl. Phys. A* **78**, 311-314 (2004).
- Cerofolini, G.F. , Localized adsorption on heterogeneous surfaces. *Thin Solid Films* **23**, 129-152 (1974).
- Chen, W., Duan, L., Wang, L.L., Zhu, D.Q.: Adsorption of hydroxyl- and amino-substituted aromatics to carbon nanotubes. *Environ. Sci. Technol.* **42**, 6862-6868 (2008).
- Dąbrowski, A., Podkościelny, P., Hubicki, Z., Barczak, M.: Adsorption of phenolic compounds by activated carbon – a critical review. *Chemosphere* **58**, 1049-1070 (2005).
- Deryło-Marczewska, A., Mirosław K., Marczewski A.W., Sternik D.: Studies of adsorption equilibria and kinetics of o-, m-, p-nitro- and chlorophenols on microporous carbons from aqueous solutions. *Adsorption* **16**, 359-375 (2010).
- Fernandez, E., Hugi-Cleary, D., Lopez-Ramon, M.V., Stoeckli, F.: Adsorption of phenol from dilute and concentrated aqueous solutions by activated carbons. *Langmuir* **19**, 9719-9723 (2003).
- Fowler, R.H., Guggenheim, E.A.: *Statistical Thermodynamics*, Cambridge, University Press, London (1949).
- Giles, C.H., Smith, D., Huitson, A.: A general treatment and classification of the solute adsorption isotherm. I. Theoretical, *J. Colloid Interf. Sci.* **47**, 755-765 (1974).
- Heuchel, M., Bräuer, P., von Szombathely, M., Messow, U., Einicke, W.D., Jaroniec, M.: Evaluation of the energy distribution function from liquid/solid adsorption measurements. *Langmuir* **9**, 2547-2554 (1993).



- Heuchel, M., Jaroniec, M.: Comparison of energy distributions calculated for active carbons from benzene gas/solid and liquid/solid adsorption data. *Langmuir* **11**, 1297-1303 (1995).
- Hua, C., Zhang, R.H., Li L., Zheng, X.Y.: Adsorption of phenol from aqueous solutions using activated carbon prepared from crofton weed. *Desalin. Water Treat.* **37**, 230-237 (2012).
- Ishimitsu, T., Hirose, S., Sakurai, H.: Microscopic acid dissociation constants of 3,4-dihydroxyphenethylamine (dopamine). *Chem. Pharm. Bull.* **26**, 74-78 (1978).
- Jaroniec, M., Madey, E.: *Physical Adsorption on Heterogeneous Solids*, Elsevier, Amsterdam (1988).
- Ji, L., Shao, Y., Xu, Z., Zheng, S., Zhu, D.: Adsorption of monoaromatic compounds and pharmaceutical antibiotics on carbon nanotubes activated by KOH etching. *Environ. Sci. Technol.* **44**, 6429-6436 (2010).
- László, K., Szűcs, A.: Surface characterization of polyethyleneterephthalate PET based activated carbon and the effect of pH on its adsorption capacity from aqueous phenol and 2,3,4-trichlorophenol solutions. *Carbon* **39**, 1945-1953 (2001).
- László, K., Podkościelny, P., Dąbrowski, A.: Heterogeneity of polymer-based active carbons in adsorption of aqueous solutions of phenol and 2,3,4-trichlorophenol. *Langmuir* **19**, 5287-5294 (2003).
- László K., Tombácz E., Kerepesi P.: Surface chemistry of nanoporous carbon and the effect of pH on adsorption from aqueous phenol and 2,3,4-trichlorophenol solutions. *Colloids Surf. A* **230**, 13-22 (2003b).
- László, K., Podkościelny, P., Dąbrowski, A.: Heterogeneity of activated carbons with different surface chemistry in adsorption of phenol from aqueous solutions. *Appl. Surf. Sci.* **252**, 5752-5762 (2006).
- Lehman, J.H., Terrones, M., Mansfield, E., Hurst, K.E., Meunier, V.: Evaluating the characteristics of multiwall carbon nanotubes. *Carbon* **49**, 2581-2602 (2011).
- Li, M.H., Hsieh, T.C., Doong, R.A., Huang, C.P.: Tuning the adsorption capability of multi-walled carbon nanotubes to polar and non-polar organic compounds by surface oxidation. *Sep. Purif. Technol.* **117**, 98-103 (2013).
- Liao, Q., Sun, J., Gao, L.: Adsorption of chlorophenols by multi-walled carbon nanotubes treated with HNO<sub>3</sub> and NH<sub>3</sub>. *Carbon* **46**, 544-561 (2008).

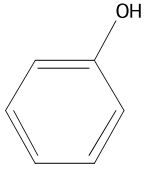
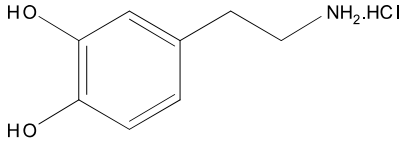
- Lin, D., Xing, B.: Adsorption of phenolic compounds by carbon nanotubes: Role of aromaticity and substitution of hydroxyl groups. *Environ. Sci. Technol.* **42**, 7254-7259 (2008).
- Marczewski, A.W.: Extension of Langmuir kinetics in dilute solutions to include lateral interactions according to regular solution theory and Kiselev association model. *J. Colloid Interf. Sci.* **361**, 603-611 (2011).
- Marczewski, A.W., Deryło-Marczewska, A., Słota, A.: Adsorption and desorption kinetics of benzene derivatives on mesoporous carbons. *Adsorption* **19**, 391-406 (2013).
- Nieszporek, K., Banach, T.: Adsorption of binary gas mixtures on strongly heterogeneous surfaces. *Sep. Sci. Technol.* **47**, 482-493 (2012).
- Nieszporek, K., Drach, M., Podkościelny, P.: Theoretical studies of hydrocarbon homologous series adsorption on activated carbons: Adsorption equilibria and calorimetry. *Sep. Purif. Technol.* **69**, 174-184 (2009).
- Pan, B., Xing, B.S.: Adsorption mechanisms of organic chemicals on carbon nanotubes. *Environ. Sci. Technol.* **42**, 9005-9013 (2008).
- Płaziński, W., Rudziński, W.: Modeling the effect of pH on kinetics of heavy metal ion biosorption. A theoretical approach based on the statistical rate theory. *Langmuir* **25**, 298-304 (2009a).
- Płaziński, W., Rudziński, W.: Modeling the effect of surface heterogeneity in equilibrium of heavy metal ion biosorption by using the ion exchange model. *Environ. Sci. Technol.* **43**, 7465-7471 (2009b).
- Podkościelny, P., Dąbrowski, A., Bülow, M.: Heterogeneity of nanoporous solids in adsorption from solutions-evaluation of energy distribution functions for adsorption in micropores of activated carbons by a comparative method. *Appl. Surf. Sci.* **196**, 312-321 (2002).
- Podkościelny, P., László, K.: Heterogeneity of activated carbons in adsorption of aniline from aqueous solutions. *Appl. Surf. Sci.* **253**, 8762-8771 (2007).
- Podkościelny, P.: The cooperative effect of the surface heterogeneity and of the lateral interactions between adsorbed molecules on adsorption of simple aromatic compounds from dilute aqueous solutions on activated carbons. *Colloids Surf. A* **318**, 227-237 (2008).
- Podkościelny, P., Nieszporek, K.: Adsorption of phenols from aqueous solutions: Equilibria, calorimetry and kinetics of adsorption. *J. Colloid Interf. Sci.* **354**, 282-291 (2011).

- Postma, A., Yan, Y., Wang, Y., Zelikin, A.N., Tjijto, E., Caruso, F.: Self-polymerization of dopamine as a versatile and robust technique to prepare polymer capsules. *Chem. Mater.* **21**, 3042 (2009).
- Radovic, L.R., Moreno-Castilla, C., Rivera-Utrilla, J.: Carbon materials as adsorbents in aqueous solutions, in: Radovic, L.R. (Ed.), *Chemistry of Physics of Carbon*, vol. **27**, pp. 227-405, Marcel Dekker, New York (2001).
- Rudziński, W., Nieszporek, K., Moon, H., Rhee, H.-K.: Fundamentals of mixed-gas adsorption on heterogeneous solid surfaces, *Heterogeneous Chem. Rev.* **1**, 275-308 (1994).
- Rudziński, W., Nieszporek, K., Cases, J.M., Michot, L.I., Villieras, F.: A new molecular probe method to study surface topography of carbonaceous solid surfaces. *Langmuir* **12**, 170-182 (1996).
- Rudziński, W., Płaziński, W.: Kinetics of metal ions adsorption at heterogeneous solid/solution interfaces: A theoretical treatment based on statistical rate theory. *J. Colloid Interf. Sci.* **327**, 36-43 (2008).
- Shen, X.-E., Shan, X.-Q., Dong, D.-M., Hua, X.-Y., Owens, G.: Kinetics and thermodynamics of sorption of nitroaromatic compounds to as-grown and oxidized multiwalled carbon nanotubes. *J. Colloid Interf. Sci.* **330**, 1-8 (2009).
- Sheng, G.D., Shao, D.D., Ren, X.M., Wang X.Q., Li, J.X., Chen Y.X., Wang X.K.: Kinetics and thermodynamics of adsorption of ionizable aromatic compounds from aqueous solutions by as-prepared and oxidized multiwalled carbon nanotubes. *J. Hazard. Mater.* **178**, 505-516 (2010).
- Soliman, E.M., Albishri, H.M., Marwani, H.M., Batterjee, M.G.: Removal of 2-chlorophenol from aqueous solutions using activated carbon-impregnated Fe(III). *Desalin. Water Treat.* **51**, 6655-6662 (2013).
- Star, A., Han, T.R., Gabriel, J.-C. P., Bradley, K., Gruner, G.: Interaction of aromatic compounds with carbon nanotubes: correlation to the Hammett parameter of the substituent and measured carbon nanotube FET response. *Nano Lett.* **3**, 1421-1423 (2003).
- Stoeckli, F., López-Ramón, M.V., Moreno-Castilla, C.: Adsorption of phenolic compounds from aqueous solutions, by activated carbons, described by the Dubinin-Astakhov equation. *Langmuir* **17**, 3301-3306 (2001).

- Terzyk, A.P.: Molecular properties and intermolecular forces - factors balancing the effect of carbon surface chemistry in adsorption of organics from dilute aqueous solutions. *J. Colloid Interf. Sci.* **275**, 9-29 (2004).
- Tóth, A., Töröcsik, A., Tombácz, E., Oláh, E., Heggen, M., Li, C., Klumpp, E., Geissler, E., László, K.: Interaction of phenol and dopamine with commercial MWCNTs, *J. Colloid Interf. Sci.* **364**, 469-475 (2011).
- Tóth, A., Töröcsik, A., Tombácz, E., László, K.: Competitive adsorption of phenol and 3-chlorophenol on purified MWCNTs, *J. Colloid Interf. Sci.* **387**, 244-249 (2012).
- Tóth, A., László, K.: Water adsorption by carbons. Hydrophobicity and hydrophilicity, in: Tascon, J.M.D. (Ed.), *Novel Carbon Adsorbents*, p. 147., Elsevier Ltd (2012).
- von Szombathely, M., Bräuer, P., Jaroniec, M.: The solution of adsorption integral equations by means of the regularization method. *J. Comput. Chem.* **13**, 17-32 (1992).
- Wang, Z., Shirley, M.D., Meikle, S.T., Whitby, R. L. D., Mikhalovsky, S.V.: The surface acidity of acid oxidised multi-walled carbon nanotubes and the influence of in-situ generated fulvic acids on their stability in aqueous dispersions. *Carbon* **47**, 73-79 (2009).
- Wiśniewski, M., Terzyk, A.P., Gauden, P.A., Kaneko, K., Hattori, Y.: Removal of internal caps during hydrothermal treatment of bamboo-like carbon nanotubes and application of tubes in phenol adsorption, *J. Colloid Interf. Sci.* **381**, 36-42 (2012).
- Woods, L.M., Badescu, S.C., Reinecke, T.L.: Adsorption of simple benzene derivatives on carbon nanotubes. *Phys. Rev. B* **75**, 155415 (2007).
- Yang, K., Wu, W., Jing, Q., Zhu, L.: Aqueous adsorption of aniline, phenol, and their substitutes by multi-walled carbon nanotubes. *Environ. Sci. Technol.* **42**, 7931-7936 (2008).

**Table 1.**

Selected physico-chemical data of the aromatic compounds (Tóth et al. 2011)

	Phenol	Dopamine
		
Molar weight (g/mol)	94.11	139.16
Solubility in water (g/l), 20 °C	82	600
p <i>K<sub>a</sub></i> , 20 °C	9.89	8.93, 10.6
$\lambda$ of detection (nm)	272.8	282.0
Cross sectional area <i>a</i> (nm <sup>2</sup> /molecule)	0.30	0.47
Supplier and purity	Merck, 99.5 %	Aldrich, 98%

**Table 2**

Parameters characterizing adsorption of phenol from aqueous solutions on original CNT-P and carboxylated form CNT-COOH (Tóth et al. 2011) obtained from the GLF, Eq. 4.\*

pH		$M$ (mmol/g)	$K'$	$\frac{kT}{v}$	$\frac{\omega}{kT}$	$\omega$ (J/mol)	$a_{GLF}^{**}$ (nm <sup>2</sup> )	<i>Error</i>	$\theta^{***}$ (%)
nom.	eq.*								
CNT-P									
pH 3	3.0	0.147	5.204	0.766	0.139	339	1.999	0.0421	15.0
not set (5.2)	6.7	0.119	3.583	0.947	0.020	49	2.470	0.0560	12.1
pH 11	8.1	0.132	5.167	0.857	0.115	280	2.227	0.0190	13.5
CNT-COOH									
pH 3	3.1	0.137	4.669	0.756	0.045	110	2.218	0.0362	13.5
not set (5.2)	4.6	0.105	4.296	0.884	0.018	44	2.894	0.0110	10.4
pH 11	7.8	0.087	4.083	0.989	0.012	29	3.493	0.1380	8.6

\*  $pH_{eq}$ : pH of the supernatant in equilibrium; \*\*  $a_{GLF} = S_{BET} / (M \cdot N_A)$ ; \*\*\* surface coverage

$\theta = 100(a \cdot M \cdot N_A / S_{BET})$  or  $\theta = 100a / a_{GLF}$

**Table 3**

Parameters characterizing adsorption of phenol from unbuffered aqueous solutions on purified MWCNTs: original CNT-PC and carboxylated form CNT-COOHC (Tóth et al. 2012) obtained from the GLF, Eq. 4.\*

$M$ (mmol/g)	$K'$	$\frac{kT}{v}$	$\frac{\omega}{kT}$	$\omega$ (J/mol)	$a_{GLF}$ (nm <sup>2</sup> )	<i>Error</i>	$\theta$ (%)
CNT-PC							
0.165	1.296	0.849	0.470	1145	1.681	0.0565	17.8
CNT-COOHC							
0.189	0.755	0.989	0.581	1416	1.643	0.1797	18.3

\*see footnote of Table 2

**Table 4**

Parameters characterizing adsorption of dopamine from aqueous solutions on original CNT-P and carboxylated form CNT-COOH (Tóth et al. 2011) from the GLF, Eq. 4.\*

pH		M (mmol/g)	K'	$\frac{kT}{\nu}$	$\frac{\omega}{kT}$	$\omega$ (J/mol)	$a_{GLF}$ (nm <sup>2</sup> )	Error	$\theta$ (%)
nom.	eq.								
CNT-P									
pH 3	4.0	0.138	8.713	0.915	0.124	302	2.130	0.2500	22.1
not set (5.3)	4.7	0.179	7.750	0.667	0.242	590	1.642	0.0839	28.6
CNT-COOH									
pH 3	3.8	0.219	16.468	0.415	0.398	970	1.388	0.1271	33.9
not set (5.3)	4.0	0.192	7.200	0.977	0.285	694	1.583	0.1037	29.7

\*see footnote of Table 2



**Table 5**

Characteristic values of the AED functions for phenol on CNT-P and CNT-COOH.

Medium	Peak location (kJ/mol)	$\varepsilon^{\max}$ (kJ/mol)	Peak height (mol/kJ)
CNT-P			
pH 3	0 – 28.56	20.85	0.124
not set (5.2)	0 – 26.26	19.47	0.146
pH 11	0 – 27.57	20.79	0.137
CNT-COOH			
pH 3	0 – 28.52	20.54	0.119
not set (5.2)	0 – 26.94	20.22	0.139
pH 11	0 – 27.96	19.91	0.140

**Table 6**

Characteristic values of the AED functions for dopamine on CNT-P and CNT-COOH.

Medium	Peak location (kJ/mol)	$\varepsilon^{\max}$ (kJ/mol)	Peak height (mol/kJ)
CNT-P			
pH 3	14.28 – 28.17	22.00	0.159
not set (5.3)	0 – 37.62	21.76	0.111
CNT-COOH			
pH 3	0 – 61.42	22.63	0.043
not set (5.3)	0 – 28.92	21.23	0.138

**Table 7**

Characteristic values of the AED functions for phenol on purified MWCNTs: CNT-PC and CNT-COOHC.

Peak location (kJ/mol)	$\varepsilon^{\max}$ (kJ/mol)	Peak height (mol/kJ)
CNT-PC		
0 – 24.14	17.79	0.146
CNT-COOHC		
0 – 21.23	16.42	0.197

## Captions for figures

**Fig. 1.** Theoretical isosteric heats of phenol adsorption from aqueous solution from Eq. 10. a) CNT-P, b) CNT-COOH

**Fig. 2.** Theoretical isosteric heats of phenol adsorption from aqueous solution on purified MWCNTs: CNT-PC and CNT-COOHC from Eq. 10.

**Fig. 3.** Theoretical isosteric heats of dopamine adsorption from aqueous solution from Eq. 10. a) CNT-P, b) CNT-COOH

**Fig. 4.** Adsorption-energy distribution functions for phenol on CNT-P (A) and CNT-COOH (B), respectively.

**Fig. 5.** Adsorption-energy distribution functions for dopamine on CNT-P (A) and CNT-COOH (B), respectively.

**Fig. 6.** Adsorption-energy distribution functions for phenol on purified MWCNTs: CNT-PC and CNT-COOHC, respectively.

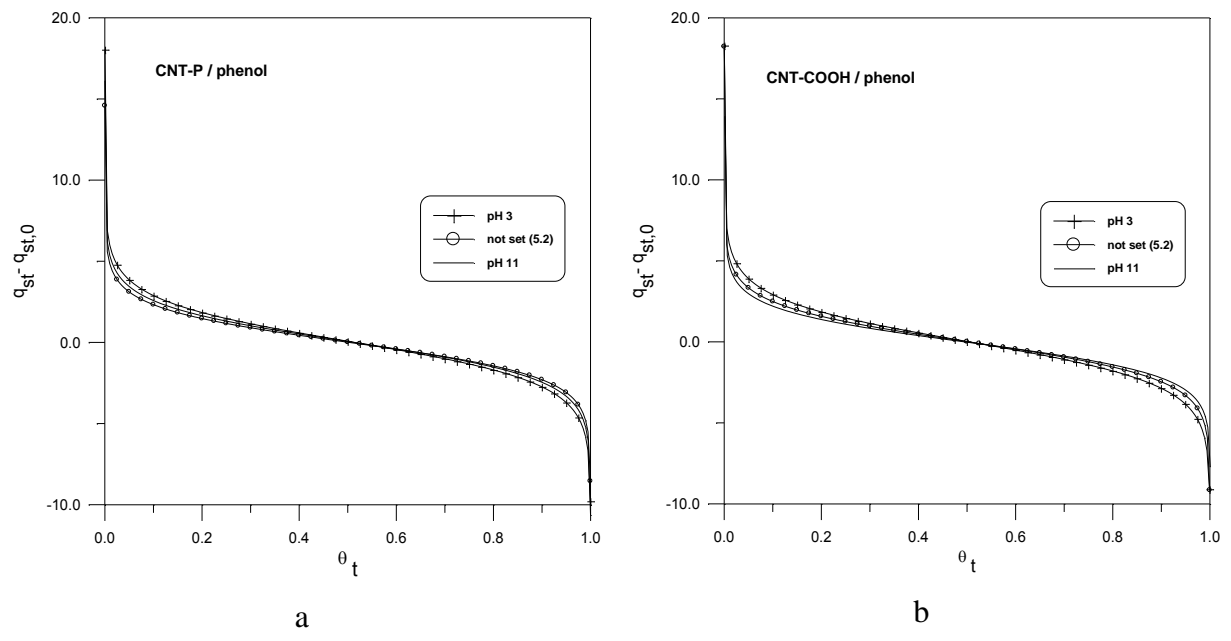


Figure 1.

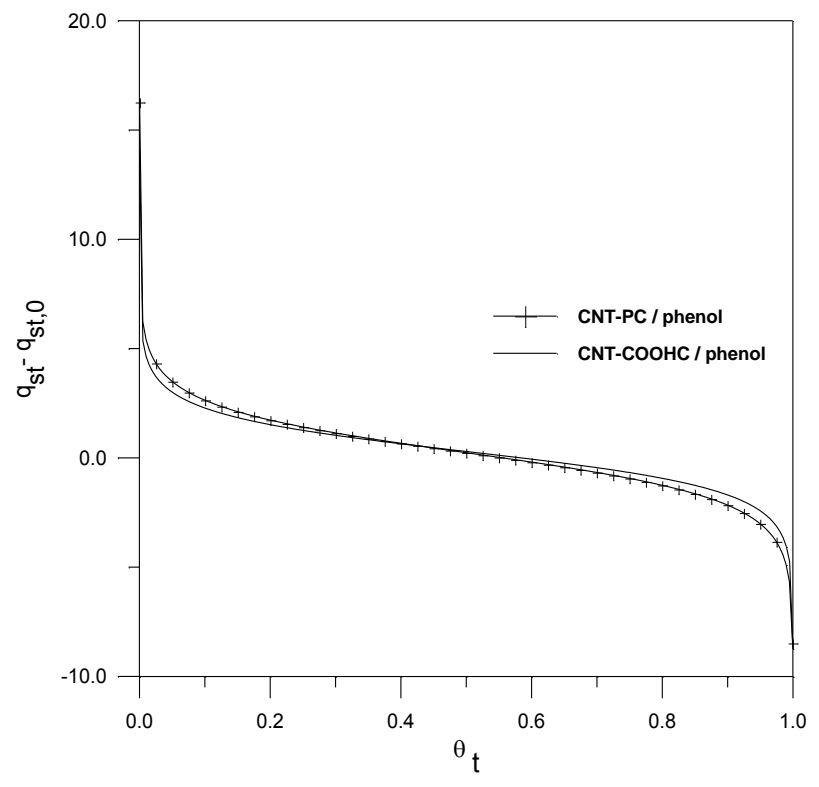


Figure 2.

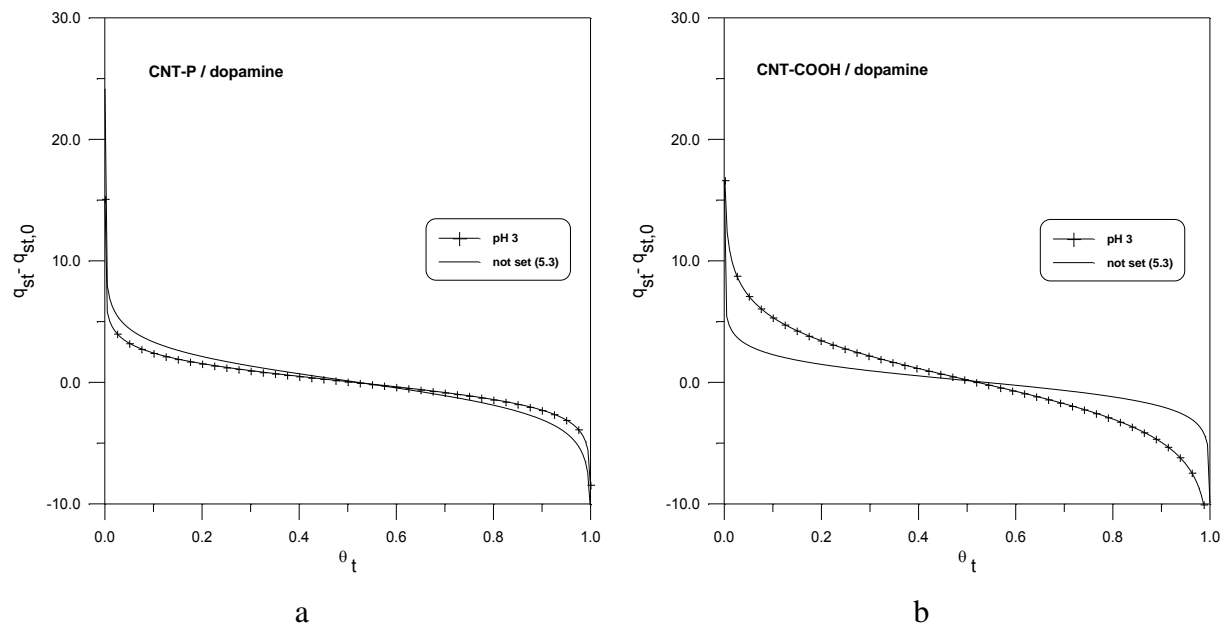


Figure 3.

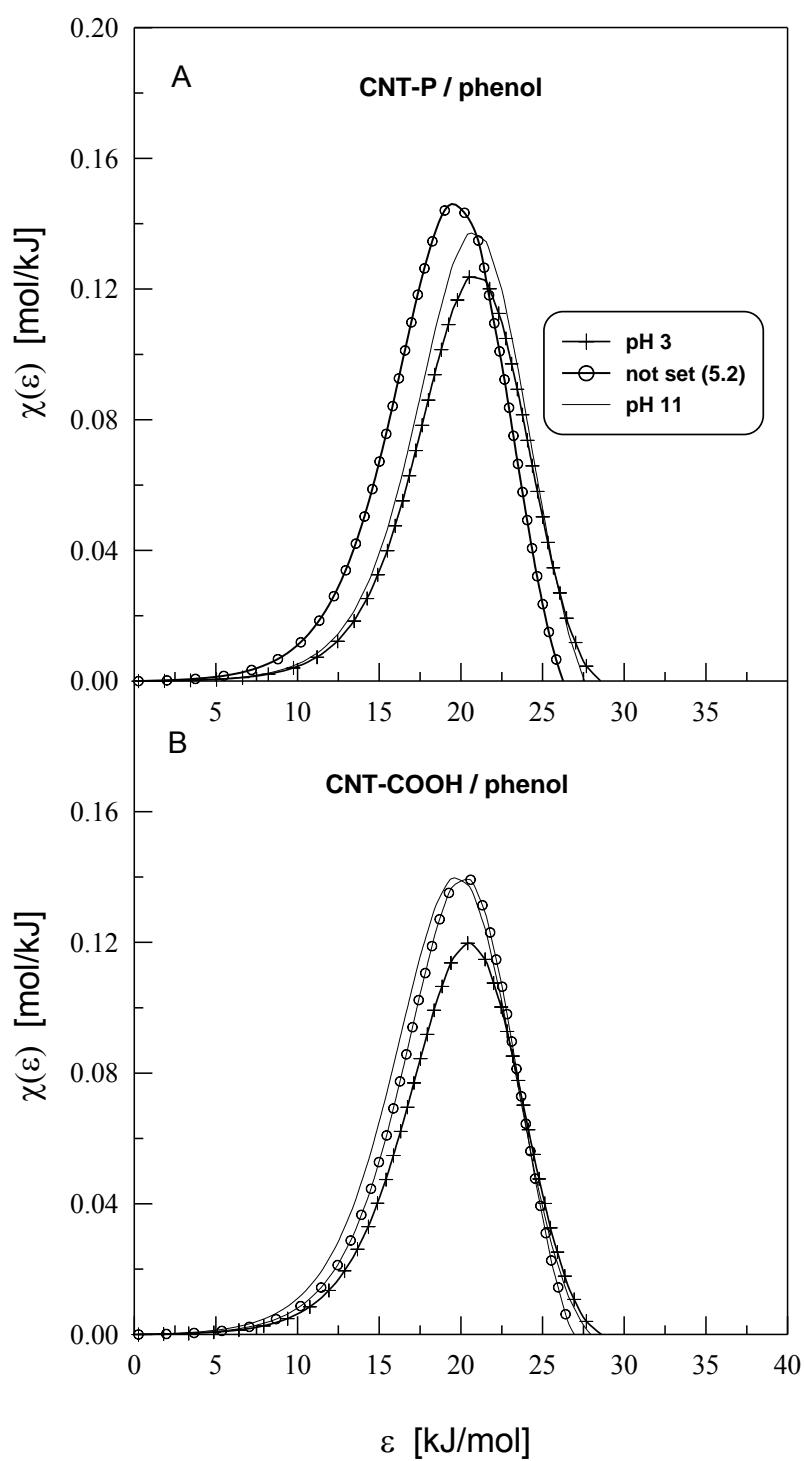


Figure 4.



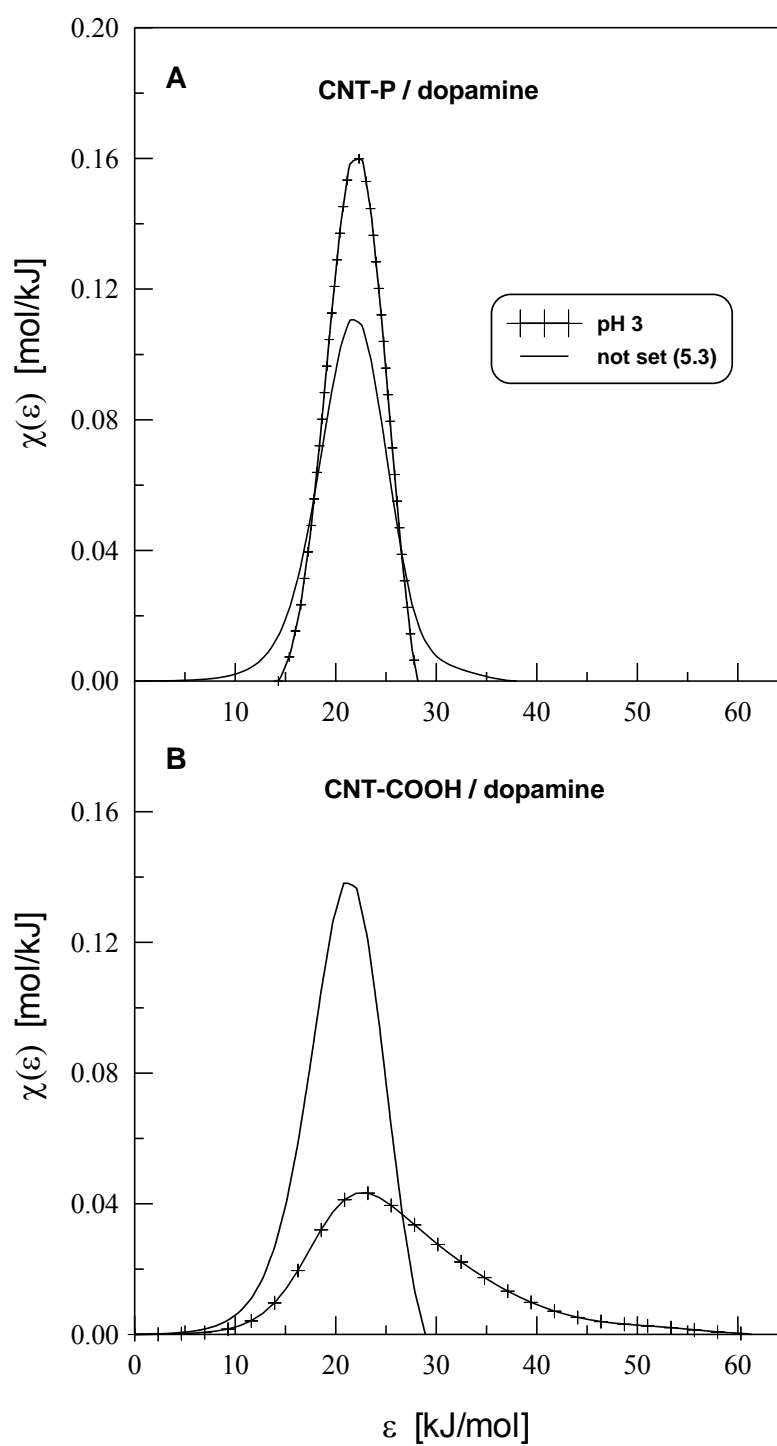


Figure 5.

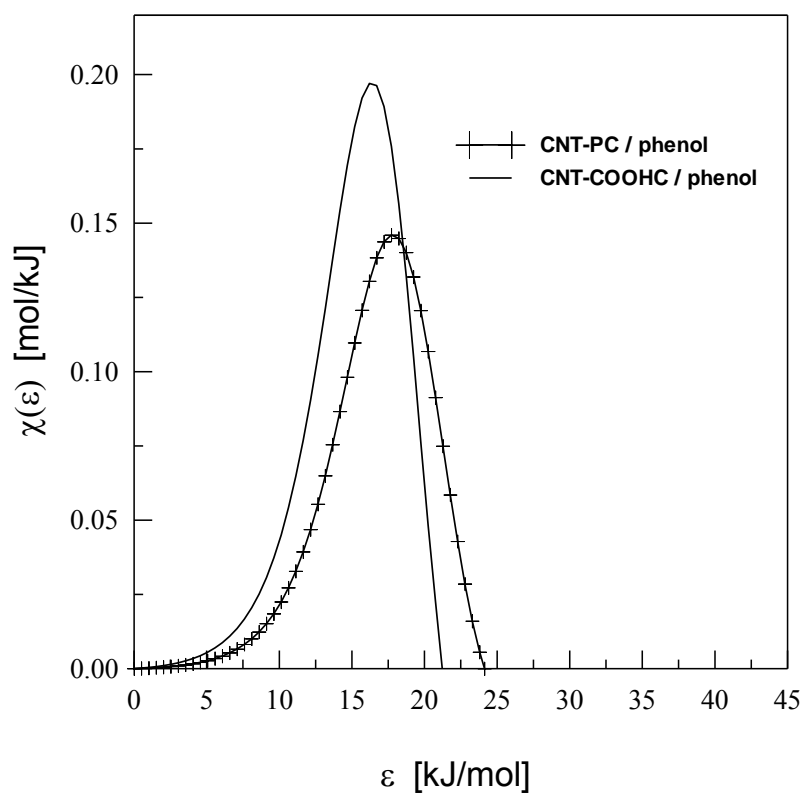


Figure 6.

### Supplementary material

Table S1. Textural characteristics of the MWCNTs (Tóth et al. 2011, 2012).\*

	$S_{BET}^*$ (m <sup>2</sup> /g)	$V_{0.95}^*$ (cm <sup>3</sup> /g)	$V_{micro}^*$ (cm <sup>3</sup> /g)	$d_{ave}^*$ (nm)	$S_{geom}^{**}$ (m <sup>2</sup> /g)
CNT-P	177	0.48	0.016	10.9	132
CNT-PC	167	0.417	0.074	10.0	
CNT-COOH	183	0.60	0.0083	13.3	120
CNT-COOHC	187	0.461	0.067	9.85	

\*  $S_{BET}$ : surface area,  $V_{0.95}$ : pore volume at  $p/p_0=0.95$  on the assumption that the pores are

filled by liquid nitrogen,  $V_{micro}$ : micropore volume,  $d_{ave}$ : average pore size,  $d_{ave} = \frac{2V_{0.95}}{S_{BET}}$ .

\*\*The geometrical surface area  $S_{geom}$ , which includes both the inner and outer surfaces, was

defined by the outer and inner radius  $R_1$  and  $R_2$  of the CNT:  $S_{geom} = \frac{2}{\rho(R_1 - R_2)} = \frac{2630}{n}$  m<sup>2</sup>/g,

where  $n$  is the number of walls. The density of the graphene layers  $\rho$  and their spacing were taken to be 2.26 g/cm<sup>3</sup> and 3.36 Å, respectively.

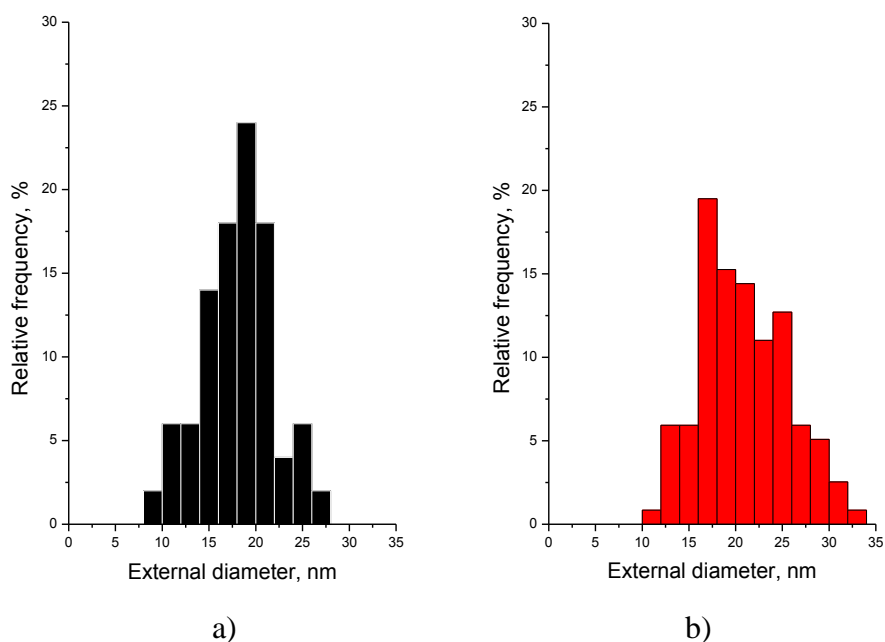


Fig. S1. Distribution of the external diameter of the as-received CNTs from HRTEM images. a) CNT-P, b) CNT-COOH

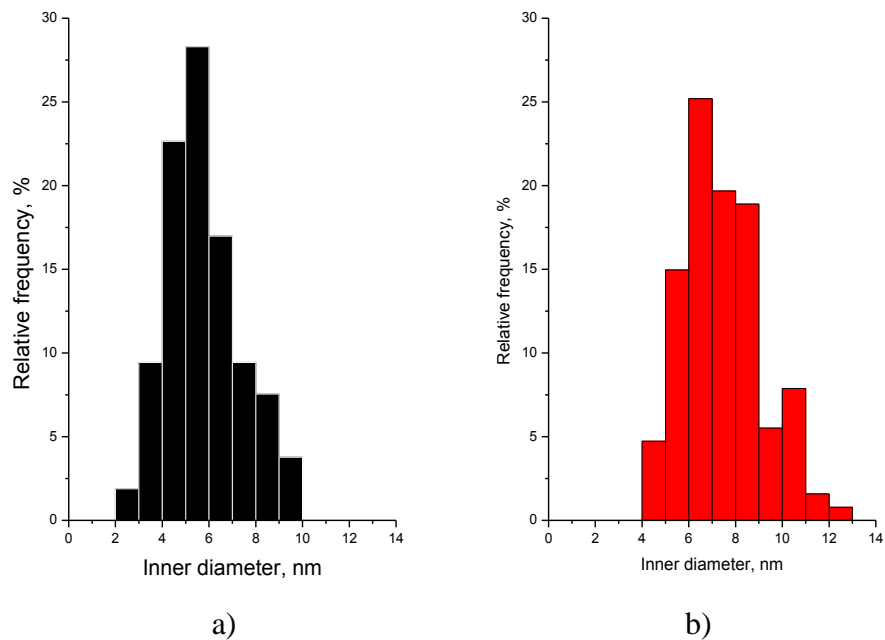


Fig. S2. Distribution of the internal diameter of the as-received CNTs from HRTEM images. a) CNT-P, b) CNT-COOH

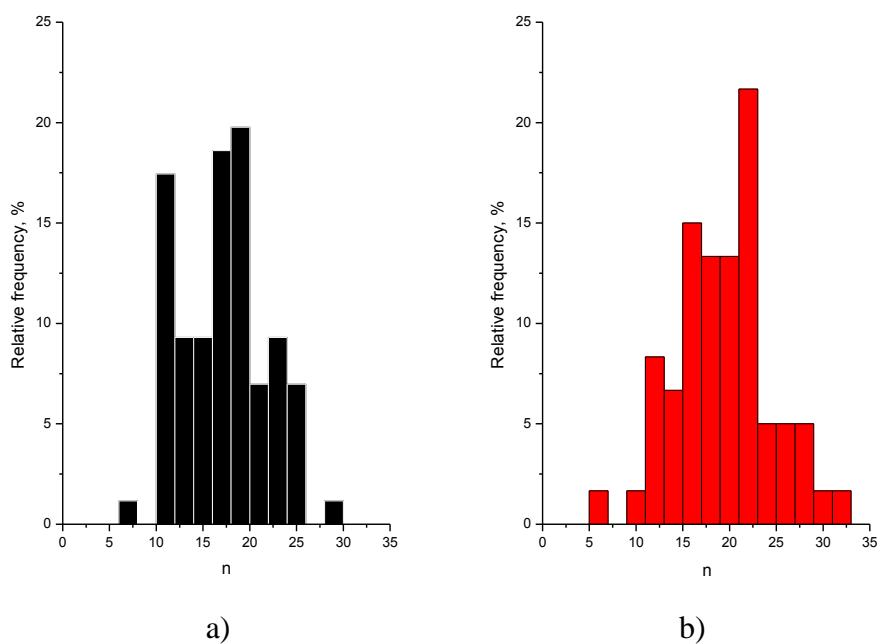


Fig. S3. Distribution of the number of walls  $n$  in the as-received CNTs from HRTEM images. a) CNT-P, b) CNT-COOH

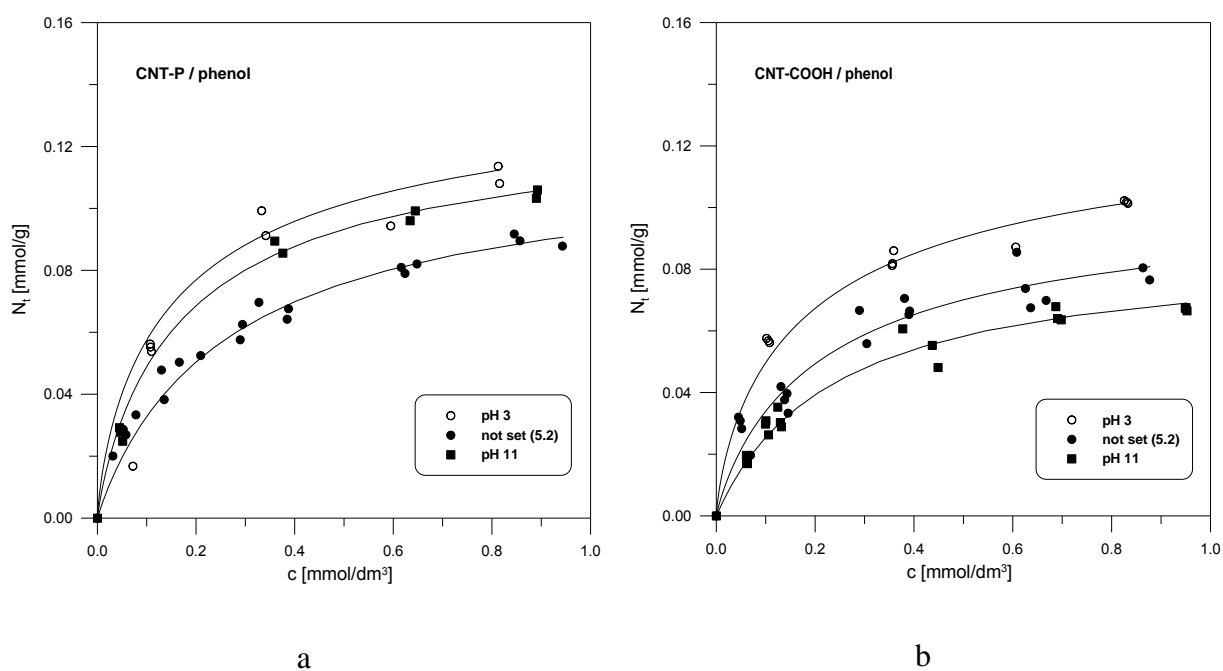


Fig. S4. Adsorption isotherms of phenol from aqueous solution at different pH values. Symbols are the measured values (Tóth et al. 2011); lines are the theoretical isotherms calculated from GLF, Eq. 4. a) CNT-P, b) CNT-COOH

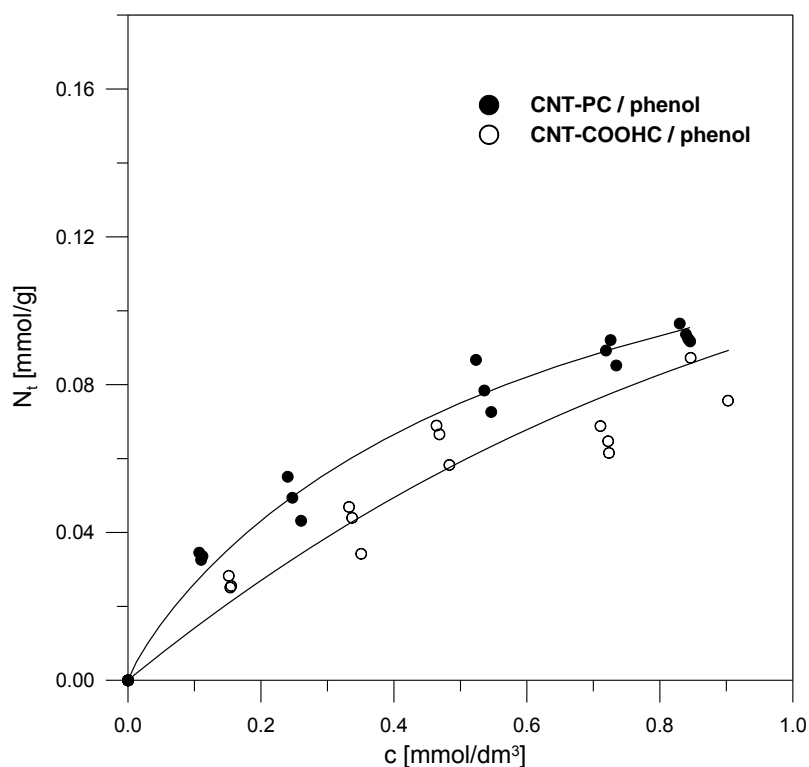


Fig. S5. Adsorption isotherms of phenol from aqueous solution on purified MWCNTs. Symbols are the measured values (Tóth et al. 2012); lines are the theoretical isotherms calculated from GLF, Eq. 4.

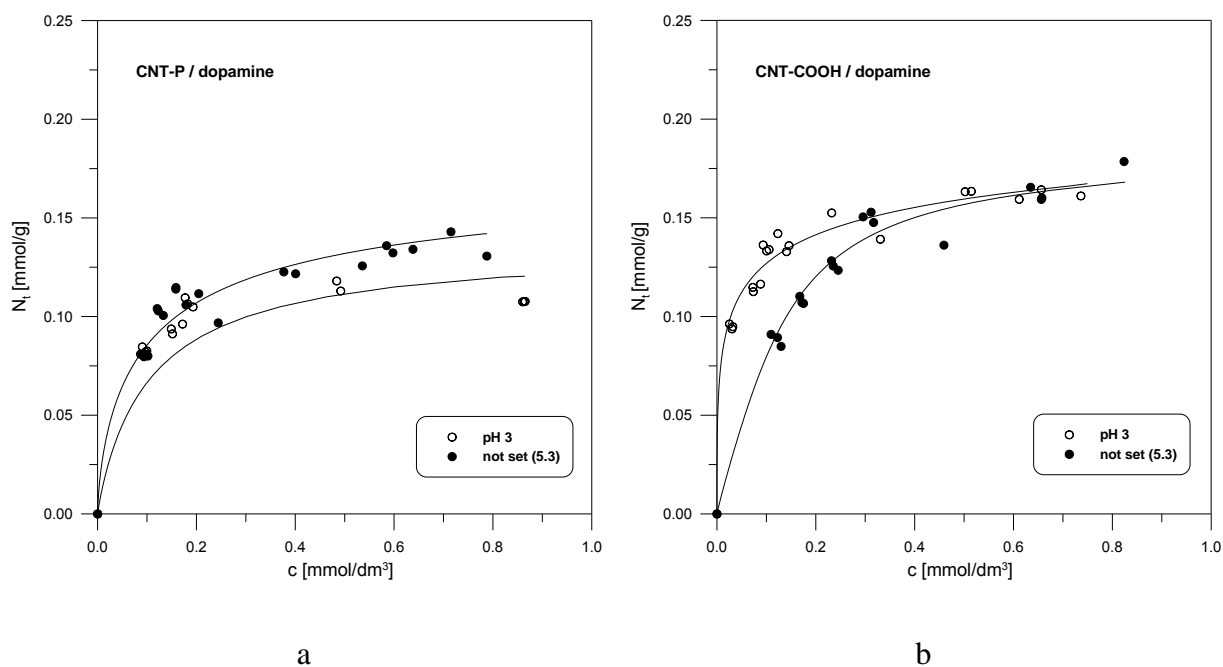


Fig. S6. Adsorption isotherms of dopamine from aqueous solution at different values of pH. Symbols are the measured values (Tóth et al. 2011); lines are the theoretical isotherms calculated from GLF, Eq. 4. a) CNT-P, b) CNT-COOH